Behavior Regulation of Adsorbed Proteins via Hydroxyapatite Surface Texture Control

Xiu-Li Dong, Hai-Long Zhou, Tao Wu,* and Qi Wang*

Department of Chemistry, Zhejiang University, Hangzhou 310027, People's Republic of China

Received: August 28, 2007; In Final Form: December 19, 2007

The influence of nanometer-scale interfaces on proteins has received much attention in recent years. The dynamic behaviors of bone morphogenetic protein-7 (BMP-7) on a series of hydroxyapatite (HAP) surface textures were investigated to explore the influence of different surface textures using molecular dynamics (MD), steered molecular dynamics simulations (SMD), and quantum mechanics calculations. It is observed that the interaction energy curve from SMD simulations can exhibit the dynamic behavior of BMP-7 in detail. Both the type and the number difference of the adsorptive residues and the intensity discrepancy of interaction, which is induced by the specific texture of the HAP surface, could be uncovered from the energy curve qualitatively and semiquantitatively in this study. The largest conformational change occurs in the system 010+a. The quantum mechanics calculations suggest that there is a phenomenon of electron transfer from HAP to the groups of BMP-7 during the adsorption process. These findings suggest that surface-engineering techniques could be employed to directly control the texture of HAP surfaces in order to regulate the behavior of a protein adsorbed onto the nanometer-scale interface.

Introduction

The interaction between proteins and nanometer-scale inorganic materials has been the subject of extensive investigation recently because of its fundamental and practical importance in the fields of biomaterials, biosensors, biofuel cells, and biomineralization.[1] It has been observed that proteins would initially be adsorbed from the bodily fluid onto the surface of implanted material and then control the subsequent cell adhesion before osteoblasts (or other cells) are adhered. Many studies have demonstrated the complexities of protein adsorption and the influence of protein adsorption on cellular response.[2,3]

Hydroxyapatite [HAP, $Ca_{10}(PO_4)_6(OH)_2$] is the predominant inorganic component of human bones and teeth. It has good biocompatibility and special surface properties as a promising biomaterial, for example, as implant materials in tissue-engineering applications and orthopedic applications and as the scaffold material for the controlled bioaffinity and controlled releasing of proteins. Although HAP is known for its binding capability to a variety of molecules, most therapeutic agents intended for bone diseases do not have a particular affinity to bone hydroxyapatite under physiological conditions.[4] This is because they lack a sufficiently high specific activity and competition from other ions, organic molecules, and proteins present in physiological milieu. In order to resolve this issue, an in-depth study is required. Recently, there are many reports on the surface textures of HAP, such as the defects,[5,6] doping,[7,8] and surface modification.[9−11] The surface nanotexture means the two-dimensional special structures of the surface at the nanoscale. In the case of HAP, it mainly results from the different Ca/P ratios. Experiments show that the model proteins ubiquitin and rhBMP-2 can be effectively immobilized noncovalently and covalently after chemical modification of a HAP ceramic surface.[12] In addition to these chemical means, surface molecular engineering, such as the atomic layer deposition (ALD),[13] may function as a better option in terms of the process industry. With the use of the established ALD technique, the surface adsorptive property of inorganic materials could be modified through the assembling of uniformly thin films atom by atom with exquisite control.[14]

Though these works improved the understanding of interactions between proteins and HAP greatly, two questions remain unsolved in experiments. First, it is a challenge for the experiments to provide the details of molecular interactions at the atomic level. Although molecular dynamics (MD) simulation is an effective method widely applied to the biomolecular systems,[15,16] it is limited to the nanosecond time scale, which is seldom long enough to the observe relevant process.[17] In contrast, steered molecular dynamics (SMD) simulation,[18,19] developed by Park and Schulten, will be a better choice. This method applies external steering forces in the right direction in order to accelerate the processes that otherwise are too slow.[17] It has been proven to be an effective way to explore the dynamic phenomena of biological macromolecular systems in relatively large time scales.[20,21] It has become a powerful tool that complements in vitro single-molecule experiments.[19]

Second, there are many factors influencing the interaction between proteins and the HAP surfaces,[22,23] such as the protein orientation, adsorptive groups, and crystal surface texture. Actually, it is difficult to investigate all these factors simultaneously. In order to explore them one by one, a series of simulations have already been carried out in our group, for example, the interacting mechanism for a certain BMP-2/HAP interface,[24] the multiple orientations of protein LRAP,[21] the dynamic behaviors of different structures of proteins (LRAP,[21] BMP-2,[24] BMP-7,[25] and fibronectin[26]), and the contribution of different adsorptive groups. It is found that the orientation of a protein molecule has great influence on the specific interaction with a certain HAP surface.[21] The carboxyl-rich structure will increase the adsorption possibility. The specific location of the carboxyl group in LRAP decides whether it can be adsorbed tightly onto the HAP surface. In addition, the electrostatic

* Corresponding authors. Fax: +86-571-87951895. E-mail: tao_wu@zju.edu.cn (T.W.), qiwang@zju.edu.cn (Q.W.).

10.1021/jp0768672 CCC: $40.75 © 2008 American Chemical Society
Published on Web 03/27/2008

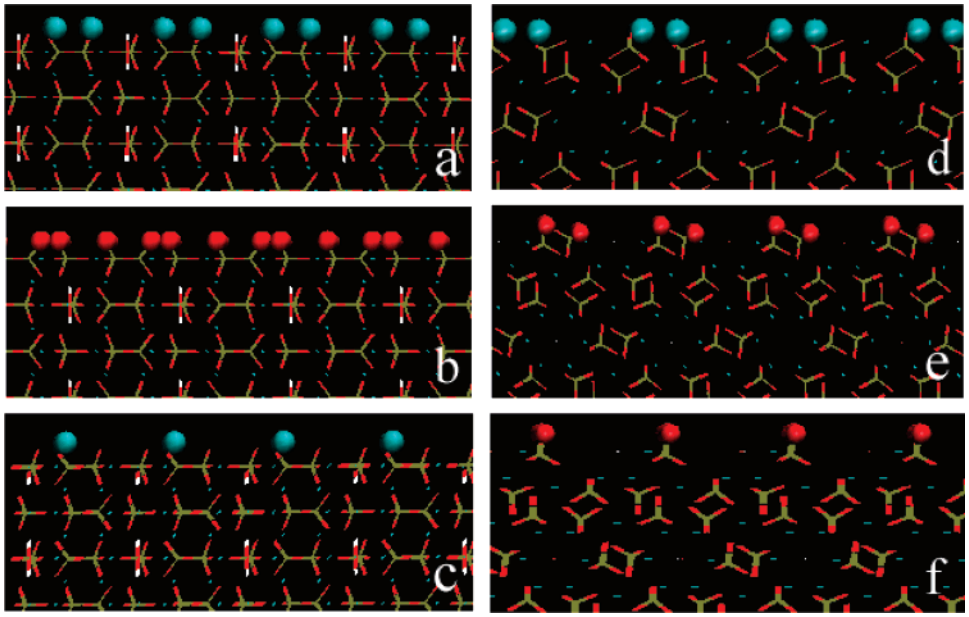

Figure 1. Textures of the six HAP surfaces investigated. Colors for atoms: O, red; P, tan; H, white; Ca, cyan. The six surfaces are (a) 001+a, (b) 001+b, (c) 001, (d) 010+a, (e) 010+b, and (f) 010.

interaction is known to be the major interaction force.[21,27] In this work, the focus is the influence of different surface textures of HAP surfaces on bone morphogenetic protein-7 (BMP-7). Therefore, based on former research, an orientation that is rich in charged groups is selected as an original model in all the systems studied. Six possible cases with different Ca/P ratio were discussed, including two natural crystal planes and four artificial HAP surfaces. It is expected to be helpful for better understanding of the nanoscale surface behaviors of proteins, the biomineralization process, and in practical applications to purposefully control the texture of the HAP surface in order to regulate the behavior of a protein adsorbed onto the nanometer-scale interfaces using PVD,[28] CVD,[29] ALD,[13] and probable ion-injection techniques.

Materials and Methods

The starting conformation of BMP-7 was downloaded from the Brookhaven protein data bank (http://www.rcsb.org/pdb/, ID = 1M4U). The original module of HAP ($P6_3/m$) was extracted from the American Mineralogist Crystal Structure database.[30] Given that the unit cell parameters for the HAP crystal are $a = b = 0.943$ nm and $c = 0.688$ nm, there are only two typical surfaces, (001) and (010). In this study, they were denoted as systems 001 and 010. In order to explore the influence of different textures of the HAP surface on proteins systemically, we obtained four other artificial surfaces with different Ca/P ratios by "cutting"[22] the HAP crystal structure parallel to the (001) and (010) surfaces. They were named as 001+a, 001+b, and 010+a, 010+b, respectively. The symbol "+a" represents that the surface is sliced with abundant of Ca^{2+} ions, whereas the symbol "+b" means that the surface is mainly composed of O atoms in PO_4^{3-} groups. The textures of these six HAP surfaces are shown in Figure 1.

First, the downloaded BMP-7 was solvated in a water box. A standard MD equilibration procedure of 1 ns was run to optimize the initial conformation. Then, six systems (001+a, 001+b, 001, 010+a, 010+b, and 010) were built up, including the equilibrated BMP-7 molecule (1741 atoms, about 2 Å away from the HAP surfaces with the same orientation) and the HAP crystal (16 632 and 17 600 atoms for 001 and 010 crystal surfaces, respectively). The area of HAP is ensured to be large enough for BMP-7 to move freely in all directions. Two Na^+ counterions were added to neutralize the systems, which is especially necessary since the BMP-7 protein carries two negative charges. In order to resemble the aqueous environment closely, the systems were completely solvated in a periodic water box of $84.9 \times 57.2 \times 115.6$ Å^3 (with the normal density, SPC model[31]). A 1 ns MD simulation was run to relax the protein in each protein−HAP complex with a time step of 2 fs in the isothermal−isobaric (NpT) ensemble ($T = 310$ K, $p = 101.3$ kPa). All the atoms can move freely during MD optimization. It ensures the possible adsorptive groups can be adsorbed completely through optimal interaction. All the simulations were performed through NAMD[32] using the Charmm27 force field[33] with the parameters[34] of HAP supplemented.

The following operations were performed for each system subsequently. First, an SMD simulation of constant velocity pulling (PCV) ($k = 2$ kcal·mol^{-1}·Å^{-2}, $v = 0.25$ Å·ps^{-1}, $t = 100$ ps) was conducted by fixing the HAP crystal and applying external steering forces uniformly on the backbone atoms of BMP-7. The external force was applied along the *c*-axis of HAP and toward the HAP surface. This process not only accelerated the adsorption process of BMP-7 onto HAP surfaces but also ensured that the possible adsorptive groups were adsorbed onto the HAP surface completely. Second, an adsorptive equilibrium MD simulation of 2 ns was performed with the same parameters mentioned above. This will ensure that the conformations obtained for the next process are stable. Third, another PCV simulation ($k = 100$ kcal·mol^{-1}·Å^{-2}, $v = 0.375$ Å·ps^{-1}, $t = 60$ ps) was carried out to study the adsorption−desorption details. The external force was also along the *c*-axis but in the direction away from the HAP surface.

On the basis of the results of MD and SMD simulations, quantum mechanics calculations were performed to investigate the atomic charge population of functional groups in the B3LYP/6-31G* level of theory using the Gaussian 03 package.[35]

Results and Discussion

1. MD Simulation of Adsorbed BMP-7. *1.1. Equilibration State.* The MD simulation has been proved to be feasible to

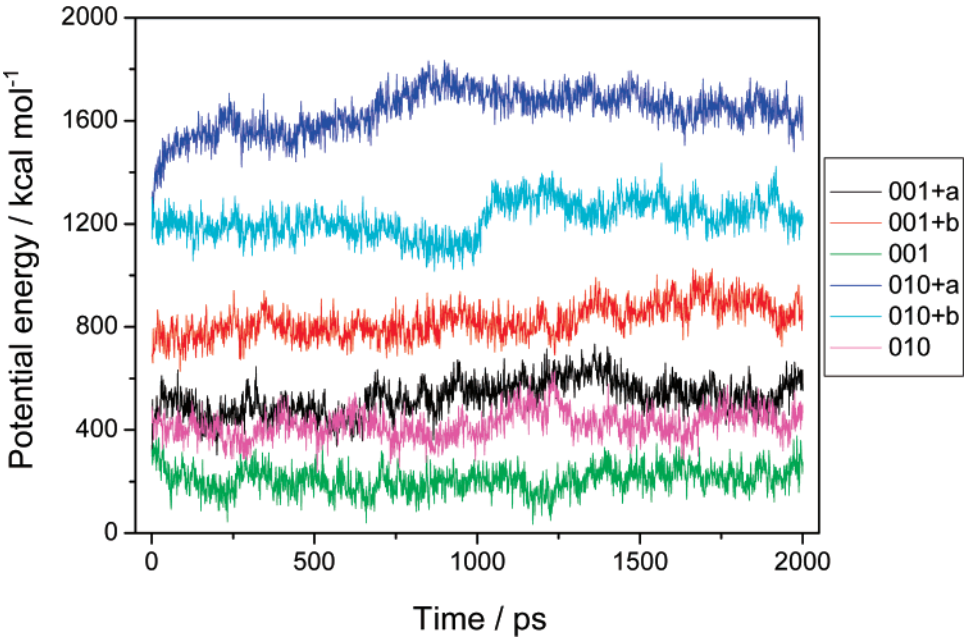

Figure 2. Potential energy of protein BMP-7 as a function of MD simulation time for the six systems investigated.

achieve equilibrium structures for bimolecular systems.[24,36] The change of potential energy[20,36] is usually employed to judge whether the system reaches equilibration or not. Here, the potential energy of BMP-7 in the last MD simulation for the six systems is shown in Figure 2. All the curves fluctuate around a definite value slightly at last, which means that they have reached the equilibration state. The conformations of protein BMP-7 were relaxed in all the directions during the 2 ns MD simulation in order to confirm that these conformations obtained after simulation are stable.

1.2. Potential Energy of BMP-7. The conformation and the function of proteins are usually greatly influenced by the surroundings. How to maintain its initial conformation and thus keep its function has been an open question for a long time. Here, the potential energy of adsorbed BMP-7 is illustrated in Figure 2 to investigate the influence of HAP and to evaluate the stability of BMP-7. As shown, the values are different in these six systems. They are about 520, 890, and 220 kcal/mol for the 001+a, 001+b, and 001 systems, respectively, whereas for systems 010+a, 010+b, and 010, they are about 1650, 1260, and 430 kcal/mol. The sequence is 010+a > 010+b > 001+b > 001+a > 010 > 001. This difference is a result of the influence of specific textures of HAP surfaces since the initial state of BMP-7 is the same. It is related with both the conformation changes of BMP-7 and the specific interaction between BMP-7 and HAP surfaces. In general, the protein will keep adjusting itself during the adsorptive process to best match the specified crystal surface. The geometric and electrostatic match between the protein and the HAP surfaces results in the change of potential energy. For systems 001+a and 010+a, the HAP surface is covered by a layer of Ca^{2+} ions. These Ca^{2+} ions attract anion groups (such as $-COO^-$) of BMP-7 strongly. The side chains with negative charges appear to be repositioned such that they match the crystal surface forming a strong Columbic interaction, which enhances the potential energy of BMP-7. As to systems 001+b and 010+b, the cases are similar, only that the outmost groups of HAP are O atoms of PO_4^{3-} ions. Other than the four artificial textures, the following discussed are two natural HAP crystal surfaces. The texture of the 001 surface is similar to that of the 001+a surface, except that the number of Ca^{2+} ions is only in half (see Figure 1). Therefore, the interaction between BMP-7 and HAP is much weaker. It induces a smaller enhancement of the potential energy. The phenomenon also holds true for system 010. In a word, the specific texture of the HAP surface exerts great influence on the potential energy of BMP-7. The lowest potential energy is in system 001. It should be noticed that the adsorption of BMP-7 on the 001+a surface is much stronger than that on the 001+b surface (to be discussed), which deviates from the sequence of potential energy. This might be related to the different sorts of adsorptive groups. Further studies are ongoing.

1.3. Conformational Change of Adsorbed BMP-7. Single-molecule measurement techniques have greatly advanced knowledge on proteins but cannot reveal enough details to be interpreted in terms of protein structure.[37] It has to be studied through MD simulations of atomic structural models.[19] To better understand the interaction between BMP-7 and the HAP, we investigated the conformational changes of BMP-7 during the adsorption process (Figure 3). The conformation in blue color is the initial state and the red one is the final state. It is found that the largest change occurs in system 010+a. The whole peptide chain of BMP-7 presents in the form of a coil with no α-helixes and β-sheets. The next one is the system 010+b, in which the secondary structure is unfolded partly and only two β-sheets remain. As to system 001+a, there is a new short α-helix formed at the C-terminus of BMP-7. But for systems 001+b, 001, and 010, no obvious changes were observed except partly breaking the intramolecular H-bonds. The results of SMD simulation show that these conformational changes are originated from the specific textures of the HAP surfaces. As the lattice matching mechanism[38,39] indicated, the structure changes to accommodate specific charges in the surface interacting with specific charged groups in the protein. When the outmost layer of the HAP surface is occupied by Ca^{2+} (systems 001+a, 001, and 010+a), the residues with negative charge (Glu and Asp) are closer to the HAP surface than those with positive charge (Lys and Arg) (see Table 1). In addition, all the adsorbed negatively charged groups are exactly repositioned on the Ca^{2+}. It is also the case in systems 001+b, 010+b, and 010. As a rule, the stronger the interaction, the larger the conformational change will be. It was found that the interaction in system 010+a is the strongest (to be discussed). Hence, the BMP-7 underwent

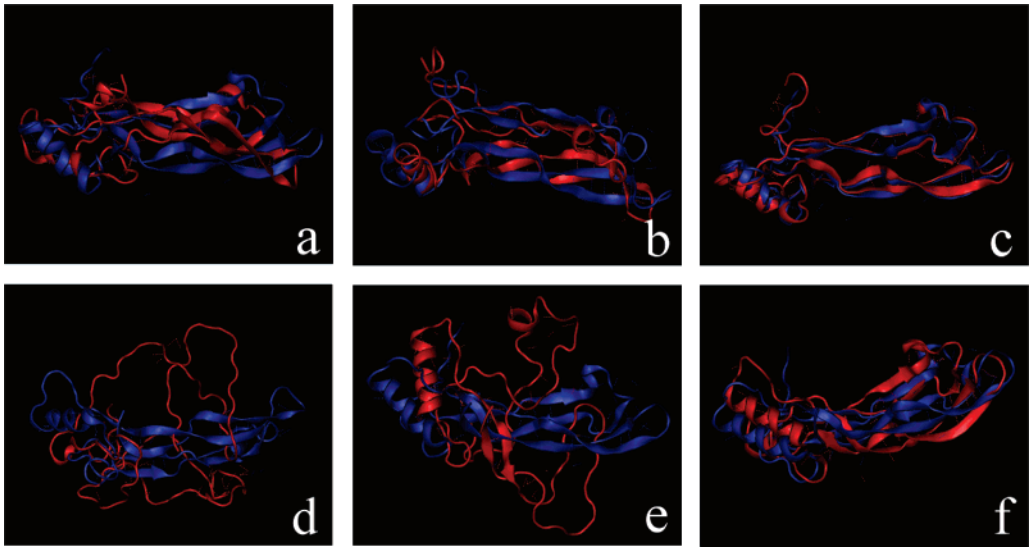

Figure 3. Conformational changes of BMP-7 by adsorption onto the HAP surfaces for the six systems through MD simulations. The ones in blue color are the initial states (actually the same state, but a little different owing to the different view angles), and the red ones are the final states. The six surfaces are (a) 001+a, (b) 001+b, (c) 001, (d) 010+a, (e) 010+b, and (f) 010. Because of the influence of the textures of HAP surfaces, the largest conformational change occurs in system 010+a (d), where all the α-helix and *β*-sheet secondary segments were totally unfolded. In system 001 (c), the protein's secondary structure is preserved the best.

TABLE 1: Distance from the HAP Surface for the Charged Groups of BMP-7 in the Equilibration Conformation

	001+a	001+b	001	010+a	010+b	010
Residues with Negatively Charged Groups						
Glu28	28.153	29.412	12.481	24.358	41.412	24.124
Glu42	2.255	23.034	2.907	1.963	38.142	25.255
Glu60	1.973	21.931	2.972	2.533	50.199	27.173
Glu68	13.091	26.383	13.924	15.100	44.621	26.959
Glu70	20.389	30.793	20.850	11.213	45.716	22.817
Glu97	15.129	41.405	32.729	18.774	56.031	29.443
Asp33	18.196	17.428	17.724	12.738	33.358	18.681
Asp49	8.224	30.274	8.634	2.831	55.547	33.570
Asp54	2.549	28.193	10.803	5.879	58.745	33.833
Asp118	9.246	18.910	21.226	12.960	36.117	24.965
Asp119	1.998	25.296	22.917	15.788	35.642	30.801
Residues with positively Charged Groups						
Lys39	14.525	6.689	7.123	21.807	17.698	9.089
Lys40	16.045	8.866	9.019	15.584	22.857	12.495
Lys101	24.096	22.762	22.781	41.974	33.338	19.040
Lys126	23.654	6.050	23.200	48.745	2.311	8.247
Lys127	27.973	3.574	18.442	51.890	1.411	5.804
Arg35	29.083	5.560	16.313	26.024	16.221	5.290
Arg48	5.471	23.666	9.289	13.841	46.591	27.768
Arg129	29.785	2.747	25.467	52.812	2.357	5.656
Arg134	30.662	3.378	14.774	37.887	10.969	3.135

the largest conformational changes. It is also interesting that the conformational change in the three 010 systems is larger than that in the corresponding 001 systems; further investigation of its mechanism is needed in the future. As widely accepted, the function of the protein is determined by its conformation. The bioactivity of BMP-7 on the 010+a HAP surface might be decreased when the unfolding effects of surfaces are too strong. In other words, the bioactivity might be preserved the best on the 001 surface. A similar effect was observed in the research of Si-doped HAP surfaces in our group. However, experimental evidence is needed to verify the relationship between the conformational changes and the bioactivity of proteins. To sum up, the conformation of BMP-7 is greatly influenced by the texture of the HAP surface, which might be closely related with its bioactivity. We would like to point out that this type of conformation-dependent phenomenon between the secondary structures of peptides and the specific crystal surface characteristics has also been testified by the circular dichroism spectra experiments recently.[40]

2. SMD Simulation of the Desorption Process. *2.1. Interaction Energy.* The behaviors of protein on a solid surface are the key to the development of biotechnology, nanotechnology, and biomaterials. The detailed mechanistic understanding of the BMP-7/HAP surface interaction in this study will be of practical value in these fields. It is found that the change of the time-dependent interaction energy, $E_{int}(t)$, from SMD simulation can provide us plenty of information on the interaction details. It is effective to distinguish the influence of different textures of the HAP surface in this study. The $E_{int}(t)$ are plotted in Figure 4; it is defined as follows:

$$E_{int}(t) = P_{HAP+BMP-7}(t) - P_{HAP}(t) - P_{BMP-7}(t) \qquad (1)$$

where $E_{int}(t)$ stands for the interaction energy between BMP-7 and HAP at time t and $P_{HAP+BMP-7}(t)$, $P_{HAP}(t)$, and $P_{BMP-7}(t)$ are the potential energy of HAPplus BMP-7, HAP, and BMP-7, respectively.

The curves of adsorptive distance (away from the HAP surface) versus SMD simulation time are shown in Figure 5. Considering that there are 11 negatively and 9 positively charged groups in BMP-7, it would be interferential if all of them were shown in figures for each system. As reported,[36] the distance of 5 Å is conventionally taken as the upper limit for the adsorptive distance with the crystal surface. Thus, only charged groups whose adsorptive distance is less than 5 Å are shown in Figure 5.

The six systems exhibit different interaction energy curves. Each inflection of the energy−time curve is ascribable to a particular molecular event, which mainly corresponds the desorption of the adsorbed residues here. For example, there are two obvious inflections (about 18 and 48 ps) in Figure 4e. It means that there are two sets of residues desorbed. That can be proved from the distance change of adsorptive residues (Figure 5) clearly. The distance of Arg129 increased dramatically from the time around 18 ps (Figure 5e). It indicates that this adsorbed residue began to be desorbed at this point. The flat from 0 to 18 ps implies that the adsorptive residues of Arg129 are absorbed onto the HAP 010+b surface tightly. Then,

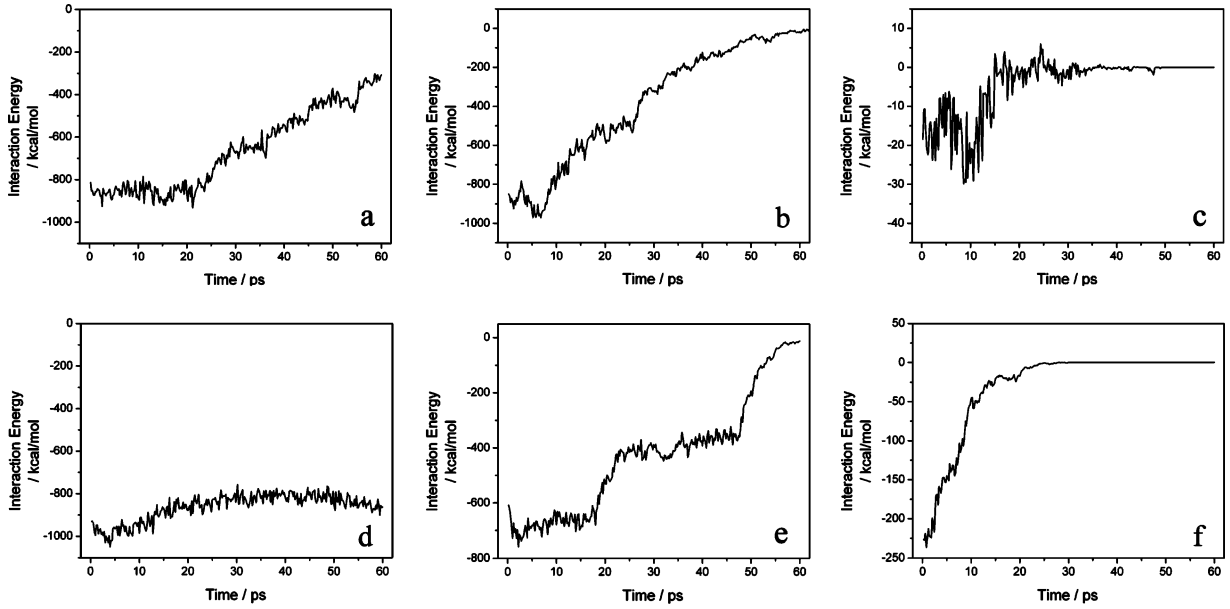

Figure 4. Interaction energy as a function of SMD simulation time for the six systems. The six surfaces are (a) 001+a, (b) 001+b, (c) 001, (d) 010+a, (e) 010+b, and (f) 010.

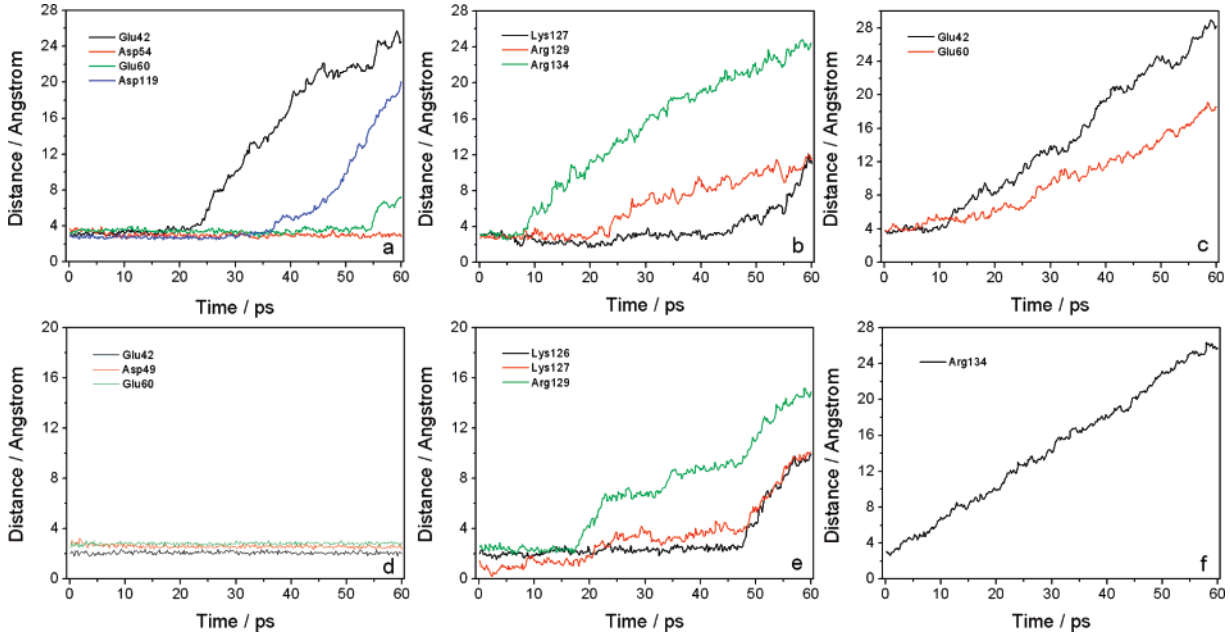

Figure 5. Distance changes as a function of SMD simulation time for the groups (marked by colored balls in Figure 6) close to the HAP surface. The six surfaces are (a) 001+a, (b) 001+b, (c) 001, (d) 010+a, (e) 010+b, and (f) 010.

it began to be desorbed from 18 ps under the external force as we have designed. Similarly, the desorption time of the other two adsorptive residues (Lys126 and Lys127) are about 48 ps. Correspondingly, there is an apparent inflection in the energy curve of Figure 4e. It is noticed that the second inflection occurred about 30 ps later than the first one. It suggests that the interaction of the second set of adsorptive residues with the HAP 010+b is much stronger than the interaction of the first one. There are two reasons. First, the second set of adsorptive residues includes two residues (Lys126 and Lys127), whereas only Arg129 is found in the first set. Second, the functional groups of Lys126 and Lys127 are $-NH_3^+$, whereas it is $-C(NH_2)_2^+$ for Arg129. The interaction between $-NH_3^+$ and PO_4^{3-} has been proved stronger than that between $-C(NH_2)_2^+$ and PO_4^{3-} ions.[26] From the time of 48 ps, the interaction energy of the 010+b system decreases sharply, and it reached zero quickly. It shows that there is no residue adsorbed onto the HAP surface any more. It is worthwhile to notice that the change of the interaction energy is exactly in consistency with the distance change of the adsorptive residues. Moreover, the interactions between these two sorts of adsorptive residues and the HAP 010+b surface are both electrostatic interactions. Therefore, it could be concluded that the electrostatic interaction is the main interaction mechanism between protein BMP-7 and the 010+b HAP surface. Similar phenomena were observed in the other five systems. In Figure 4a, there are three inflections at about 22, 36, and 55 ps; therefore, there should be three sets of residues desorbed at these points. They are Glu42, Asp119, and Glu60 (Figure 5a), respectively. There is one more thing in system 001+a, that the interaction energy is still more than 200 kcal/mol. It means that there still should be residues absorbed tightly onto the HAP 001+a system. Figure 5a shows that it is the fact indeed, and this absorbed residue is Asp54. The interaction energy of the 010+a system (Figure 4d) maintains no less than

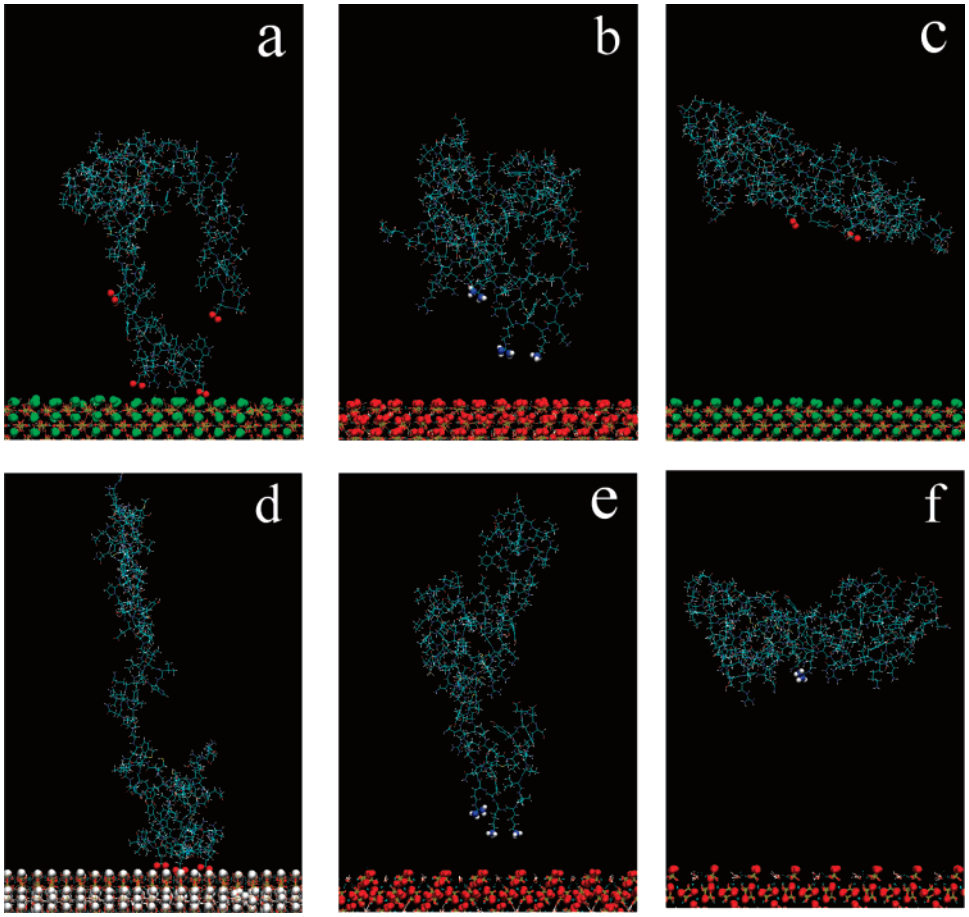

Figure 6. Snapshots of final states during the 60 ps SMD simulation for the six systems. Colors for atoms: O, red; N, blue; H, small white; C, cyan; Ca1, green; Ca2, larger white. The six surfaces are (a) 001+a, (b) 001+b, (c) 001, (d) 010+a, (e) 010+b, and (f) 010.

800 kcal/mol until the end of the SMD simulation. It shows a very strong interaction between BMP-7 and the HAP 010+a surface. Moreover, there should be no residues adsorbed because no inflections are found. From Figure 5d, this is the case that three residues (Glu42, Asp49, and Glu60) are adsorbed tightly until the time is 60 ps. In the case of the 010 system, the energy curve increases linearly, and it reaches 0 kcal/mol quickly (Figure 4f), which is in good consistency with the fact that there are not any residues adsorbed (Figure 5f).

The interaction energy exhibits the interaction intensity in different systems. As Figure 4 shows, the difference of interaction energy induced by the specific texture of HAP is as large as 1000 kcal/mol. However, the difference induced by the different orientations of the protein fibronectin is not more than 500 kcal/mol.[26] It shows that the influence of HAP surface texture is more important. The largest interaction energy is in the 010+a system, where the value is more than 800 kcal/mol during the whole 60 ps, and it is more than 1000 kcal/mol initially. This largest interaction induces the largest conformational changes in this system (Figure 3d) as discussed above. Similarly, the value of $E_{int}(t)$ in the 001 system is the smallest (not more than 30 kcal/mol). The weak interaction cannot result in much change in the structure of BMP-7. It is agreed with the experimental results that the peptide of statherin does not exhibit a large change in structure on the natural HAP surface.[41] Therefore, the conformation is best preserved in this system (Figure 3c). It is noticed that there are three adsorptive residues in both systems 010+a and 010+b; however, the deviation of the interaction energy at the initial point is apparent, which is about 300 kcal/mol. This difference implies that the interaction of adsorptive residues in these two systems must be different. It can be verified from Figure 6, which shows that the adsorptive groups are $-COO^-$ (red balls) and $-NH_3^+$ or $-C(NH_2)_2^+$ (balls in blue and white). In fact, the interaction between $-NH_3^+$ or $-C(NH_2)_2^+$ and PO_4^{3-} is weaker than that between $-COO^-$ and Ca^{2+} ions.[26]

To sum up, the interaction energy curves exhibit the adsorption−desorption behaviors of proteins on the HAP surface very well. The larger interaction energy indicates stronger interaction. When an inflection occurs in the $E_{int}(t)$−time curve, there will be a set of functional groups desorbed.

2.2. Details of Desorption Behavior of BMP-7. Detailed study shows that the difference of the interaction energy curve is related with both the type and the number of the adsorptive groups. The snapshots for the final states of SMD simulations are illustrated in Figure 6, where the groups that are close to the HAP surface in the equilibration states are present as balls (colors for atoms: O, red; N, blue; H, small white; C, cyan; Ca1, green; Ca2, larger white).

Under the influence of the specific textures of HAP surfaces, two sorts of adsorptive groups are found: negatively charged $-COO^-$ and positively charged $-NH_3^+$ or $-C(NH_2)_2^+$. Usually, only one of them was discussed in most literature.[42,43] This binding preference may be explained in terms of the lattice matching[38,39] between the adsorbed residues and the appropriate HAP crystal surface. As discussed above, Ca^{2+} cations occupy the outmost layer of the HAP surface in systems 001+a, 010+a, and 001, which results in the fact that $-COO^-$ groups are prone to be adsorbed. In systems 001+b, 010+b, and 010, the groups on the HAP surface are PO_4^{3-} anions; therefore, the corre-

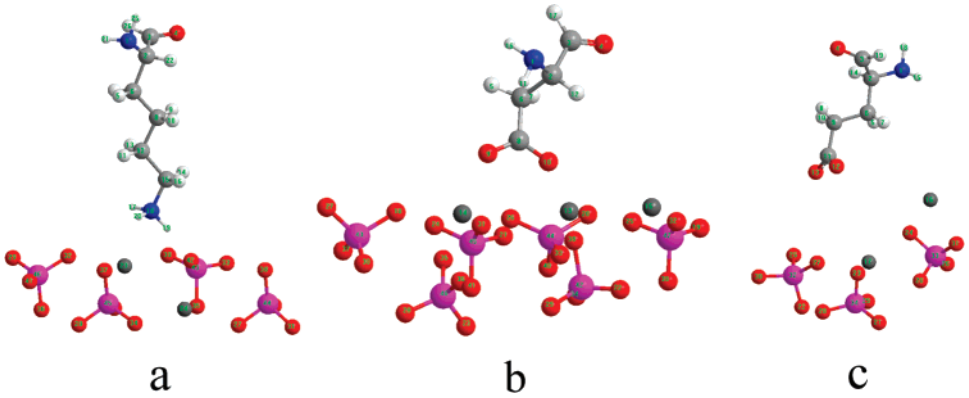

Figure 7. Structures calculated using the G03 package: (a) Lys126 in system 010+b; (b) Asp49 in system 010+a; (c) Glu60 in system 001. Colors for atoms: O, red; N, blue; H, white; C, light gray; Ca, heavy gray.

sponding adsorptive groups are $-NH_3^+$ and $-C(NH_2)_2^+$. The residues that contain these adsorptive groups are determinate. The $-COO^-$ ions only belong to residues Glu and Asp in all these six systems. It is reasonable because they are the only two acidic amino acids among the 20 amino acids. The carboxyl group will be in the form of $-COO^-$ ions when pH equals 7.0. As to the marked $-NH_3^+$ and $-C(NH_2)_2^+$, they all are part of residues Lys or Arg, whose isoelectric points are 9.59 and 11.15, respectively. It is worthwhile to notice that only these four types of residues are obviously close to the HAP surface among all the 112 residues in BMP-7. Especially, this is also the case for the two natural surfaces. Therefore, these four types of residues should be considered particularly when talking about the interaction between BMP-7 and the HAP crystal. It might be realizable to solicit a desired biological response by regulating these four types of residues of proteins.

The number of adsorptive residues also plays great importance on the interaction energy. It is sometime positively correlated with the ion density or the net charges on the specific HAP surface. For system 001+a, the density of surface Ca^{2+} ions is twice that in system 001. Correspondingly, there are four residues (Glu42, Asp54, Glu60, and Asp119) adsorbed onto the HAP surface; however, there are only two (Glu42 and Glu60) in system 001 (Figure 6). With respect to systems 010+b and 010, similar results are observed. The net charges of the 010+b surface are twice that on the 010 surface; thus, the interactive residue in system 010+b is three (Lys126, Lys127, and Arg129), whereas there is only one residue (Arg134) close to the HAP surface in system 010. Similarly, the density of Ca^{2+} in 001 is smaller than that in system 010+a, so the residues close to the HAP surface in system 001 are one less than that in system 010+a. As to the 001+b surface, the density of PO_4^{3-} is similar to that in 010+b (Figure 1, parts b and e), three interactive residues being observed in both cases (Lys127, Arg129, and Arg134 in system 001+b, and Lys126, Lys127, and Arg129 in system 010+b).

In this study, four types of groups are observed firmly adsorbed onto the HAP surface; however, it does not mean that they must be adsorbed effectively under any condition. First, the interaction is influenced by the specific texture of the HAP surface. For example, the distances of residue Glu42 from the HAP surface are less than 5 Å in both system 001 (2.907 Å) and system 010+a (2.255 Å); however, it forms a strong interaction with the HAP crystal only in the latter system (Figure 5). That is because the density of surface Ca^{2+} ions in system 001+a is larger than that in system 001. It is very easy for Glu42 in system 001+a to be located at the position of the Ca^{2+} lattice, as shown in Figure 6a. In addition, the large number of Ca^{2+} ions induces the strong interaction between Glu42 and the HAP 001+a surface, which makes this residue adsorbed tightly. In contrast, the interaction in 001 is much weaker, and no effective adsorption was formed. Second, the distance from the functional groups to the HAP surface is also one of the important factors. For instance, only groups Glu42 and Glu60 are adsorbed among the six Glu residues in the 010+a system. That is the result of the different initial distances (Table 1). As we know, the Coulombic force is in inverse proportion to the square of the distance. If the distance is too far (like Glu28, Glu68, Glu70, and Glu97), the force is not strong enough to form adsorption. The last but not the least, the local structure where a residue is located is important. In general, the rigid structure, such as the α-helixes, will resist the reposition of the charged residues. It is now well recognized that the osteoblasts are preferentially adhered to specific amino acid sequences such as the Arg-Gly-Asp (RGD) loop in adsorbed proteins.[3,44] Briefly, both the specific texture of the HAP surface and the location of a residue influence the protein−HAP interaction. When the distance is small, the lattice matching mechanism plays the key role; otherwise, the electrostatic interaction will be more influential.

In conclusion, the way of "cutting" changes the types of HAP surface ions and increases the density of ions or the quantity of net charges in a given area. These specific textures of the HAP surface greatly influence the type, the number, the adsorptive time, and the intensity of interaction of adsorptive residues. All of these can be well exhibited in the interaction energy curve qualitatively and semiquantitatively. It is expected that the adsorption−desorption behaviors of BMP-7 or other proteins might be regulated through modifying the HAP surface. Thus, it might be possible to control the release of protein or peptide medicines and to enhance the separation and purification of proteins.

3. Quantum Mechanics Calculation. Given that the interaction of BMP-7 with HAP is mainly through the electrostatic force, it will be interesting to investigate the change of Mulliken atomic charge (AC) population for functional groups before (B) and after (A) their adsorption onto the HAP surface. The systems studied are selected as 010+a, 010+b, and 001, where the conformational change of BMP-7 is the largest two and the smallest one. The change is defined as follows:

$$\Delta AC = AC_A - AC_B \quad (2)$$

where AC_A and AC_B stand for the Mulliken atomic charge population after and before adsorption, respectively. The corresponding structures are shown in Figure 7.

As shown in Table 2, in the B3LYP level of theory, the Mulliken atomic charge population of residue Lys126 in system

TABLE 2: Mulliken Atomic Charges (AC) of Lys126 in System 010+b, $\Delta AC = AC_A - AC_B$

	AC_B	AC_A	ΔAC
1N	−0.712	−0.661	0.051
2C	−0.024	0.028	0.052
3C	0.229	0.100	−0.129
4O	−0.362	−0.612	−0.250
6C	−0.304	−0.239	0.065
8C	−0.263	−0.242	0.021
12C	−0.313	−0.280	0.033
15C	−0.202	−0.171	0.031
17H	0.435	0.400	−0.035
18N	−0.719	−0.686	0.033
19H	0.440	0.478	0.038
20H	0.425	0.372	−0.053
NH_3^+	0.581	0.564	−0.017
Lys126	1.000	−0.248	−1.248
HAP	−8.000	−6.752	1.248

TABLE 3: Mulliken Atomic Charges (AC) in Systems 010+b, 010+a, and 001, $\Delta AC = AC_A - AC_B$

	AC_B	AC_A	ΔAC
	System 010+b		
$-NH_3^+$	0.581	0.564	−0.017
Lys126	1.000	−0.248	−1.248
HAP	−8.000	−6.752	1.248
	System 010+a		
$-COO^-$	−0.732	−0.494	0.238
Asp49	−1.000	−1.850	−0.850
HAP	−12.000	−11.150	0.850
	System 001		
$-COO^-$	−0.734	−0.667	0.067
Glu60	−1.000	−1.260	−0.260
HAP	−5.000	−4.740	0.260

010+b changes obviously because of the interaction between BMP-7 and the HAP. The total charge of Lys126 changes from +1.000 to −0.248, and the charge of NH_3^+ decreases from 0.581 to 0.564. In contrast, the charge of HAP part changes from −8.000 to −6.752. This indicates that the electron-transfer phenomenon occurred during the adsorption process of Lys126 onto the HAP surface. The charges of other atoms in Lys126 also change in different degrees, except for the backbone atoms in the main chain. It is also found that this type of electronic effect influences the backbone atoms of Lys126 and results in a sharp charge change (from −0.362 to −0.612) of the atom "4O", which is at the end of residue Lys126. As shown in Figure 7a, it is the atom "19H" that interacts with the HAP surface most strongly at this time. (In our previous studies, it was found that the three H atoms of $-NH_3^+$ can alternately interact with the PO_4^{3-} group on the HAP surface through H-bonds.) Accordingly, as a result of strong electrostatic force between the $-NH_3^+$ group and the HAP surface, which makes the electronic transfer from the atom "19H" to the other two H atoms ("17H" and "20H") in this $-NH_3^+$ group, the atomic charge of "19H" increases by 0.038 after its adsorption onto the HAP 010+b surface.

For systems 010+a and 001, only the charge changes of functional groups and the corresponding HAP parts are listed in Table 3 for clarity. It is found that there is an electron-transfer phenomenon from HAP to the adsorptive residue in all these three systems. The quantity of the transferred charges in system 001 is the smallest, which is only 0.260. In contrast, the quantity is 1.248 and 0.850 in systems 010+b and 010+a, respectively. This phenomenon is consistent with the results that the interaction between BMP-7 and HAP in system 001 is the smallest. It can be presumed that the stronger the interaction, the more electrons are transferred. As to the difference between systems 010+b and 010+a, it is the relative distance between the functional groups and the HAP surface that plays the key role. For the residue Lys126 in system 010+b, the distance is about 2 Å, whereas for Asp49 in system 010+a and Glu60 in system 001, the distances are ∼3 and ∼4 Å, respectively. This shows that the closer distance will make the electron transfer much easier.

Conclusion

In this study, we explored the influence of different textures of the HAP surface on protein BMP-7 in a controlled way. It is observed that the interaction energy curve from SMD simulation can provide the dynamic behavior of BMP-7 in detail. It exhibits not only the relative interaction intensity semiquantitatively, but also the number of desorbed groups, the type of desorbed groups, and the time of desorption. Detailed studies show that the strong interaction might induce dramatic conformational changes in BMP-7. The largest conformational change occurs in system 010+a. The potential energy sequence of protein adsorbed in these six systems is 010+a > 010+b > 001+b > 001+a > 010 > 001. According to the different textures of HAP surfaces, there are only two categories of functional groups, that is, $-COO^-$ and $-NH_3^+$ or $-C(NH_2)_2^+$. The quantum mechanics calculations suggest that there is a phenomenon of electron transfer from HAP to the groups of BMP-7 during the adsorption process.

Considering that the interfaces between protein BMP-7 and HAP are various, we noticed that the orientation discussed here is not sufficient for the complete study of BMP-7−HAP interactions. As to the influence of different orientations of BMP-7, a further study is ongoing. However, the orientation of protein BMP-7 here is representative. This study provides us the probability that the specific texture of the HAP surface can be purposefully modified through surface molecular engineering. Then, the dynamic behaviors of proteins may be regulated in order to match the requirement for specific applications, such as controlled release of protein or peptide medicines, surface regulation of biomaterials, efficient separation and purification of proteins, and other applications of biomedical and industrial materials.

Acknowledgment. This work was financially supported by the National Natural Science Foundation of China (Grant Nos. 60533050 and 20503025).

References and Notes

(1) Xiong, Y. J.; Shi, L.; Chen, B. W.; Mayer, M. U.; Lower, B. H.; Londer, Y.; Bose, S.; Hochella, M. F.; Fredrickson, J. K.; Squier, T. C. *J. Am. Chem. Soc.* **2006**, *128*, 13978.

(2) Langer, R.; Tirrell, D. A. *Nature* **2004**, *428*, 487.

(3) Stevens, M. M.; George, J. H. *Science* **2005**, *310*, 1135.

(4) Gittens, S. A.; Bansal, G.; Zernicke, R. F.; Uludağ, H. *Adv. Drug Delivery Rev.* **2005**, *57*, 1011.

(5) Jäger, C.; Welzel, T.; Meyer-Zaika, W.; Epple, M. *Magn. Reson. Chem.* **2006**, *44*, 573.

(6) Peroos, S.; Du, Z.; de Leeuw, N. H. *Biomaterials* **2006**, *27*, 2150.

(7) Vandiver, J.; Dean, D.; Patel, N.; Botelho, C.; Best, S.; Santos, J. D.; Lopes, M. A.; Bonfield, W.; Ortiz, C. *J. Biomed. Mater. Res.* **2006**, *78*, 352.

(8) Feng, Z. D.; Liao, Y. M.; Ye, M. *J. Mater. Sci.: Mater. Med.* **2005**, *16*, 417.

(9) Pramanik, N.; Mohapatra, S.; Pramanik, P.; Bhargava, P. *J. Am. Ceram. Soc.* **2007**, *90*, 369.

(10) Choi, H. W.; Lee, H. J.; Kim, K. J.; Kim, H. M.; Lee, S. C. *J. Colloid Interface Sci.* **2006**, *304*, 277.

(11) Lee, H. J.; Choi, H. W.; Kim, K. J.; Lee, S. C. *Chem. Mater.* **2006**, *18*, 5111.

(12) Zurlinden, K.; Laub, M.; Jennissen, H. P. *Materialwiss. Werkstofftech.* **2005**, *36*, 820.

(13) Hausmann, D.; Becker, J.; Wang, S. L.; Gordon, R. G. *Science* **2002**, *298*, 402.
(14) Kingon, A. I.; Maria, J. P.; Streiffer, S. K. *Nature* **2000**, *406*, 1032.
(15) Becker, O. M.; MacKerell, A. D.; Roux, B.; Watanabe, M. *Computational Biochemistry and Biophysics*; Marcel Dekker: New York, 2001.
(16) Bhowmik, R.; Katti, K. S.; Katti, D. *Polymer* **2007**, *48*, 664.
(17) Park, S.; Schulten, K. *J. Chem. Phys.* **2004**, *13*, 5946.
(18) Lu, H.; Schulten, K. *Biophys. J.* **2000**, *79*, 51.
(19) Sotomayor, M.; Schulten, K. *Science* **2007**, *316*, 1144.
(20) Isralewitz, B.; Gao, M.; Schulten, K. *Curr. Opin. Struct. Biol.* **2001**, *11*, 224.
(21) Chen, X.; Wang, Q.; Shen, J. W.; Pan, H. H.; Wu, T. *J. Phys. Chem. C* **2007**, *111*, 1284.
(22) Zahn, D.; Hochrein, O. *Phys. Chem. Chem. Phys.* **2003**, *5*, 4004.
(23) Zahn, D.; Hochrein, O. *Z. Anorg. Allg. Chem.* **2005**, *631*, 1134.
(24) Dong, X. L.; Wang, Q.; Wu, T.; Pan, H. H. *Biophys. J.* **2007**, *93*, 750.
(25) Zhou, H. L.; Wu, T.; Dong, X. L.; Wang, Q.; Shen, J. W. *Biochem. Biophys. Res. Commun.* **2007**, *361*, 91.
(26) Shen, J. W.; Wu, T.; Wang, Q.; Pan, H. H. *Biomaterials* **2008**, *29*, 513.
(27) Wallwork, M. L.; Kirkham, J.; Zhang, J.; Smith, D. A.; Brookes, S. J.; Shore, R. C.; Wood, S. R.; Ryu, O.; Robinson, C. *Langmuir* **2001**, *17*, 2508.
(28) Hamdi, M.; Ektessabi, A.-I. *Surf. Coat. Technol.* **2006**, *201*, 3123.
(29) Monkawa, A.; Ikoma, T.; Yunoki, S.; Ohta, K.; Tanaka, J. *J. Nanosci. Nanotechnol.* **2007**, *7*, 833.
(30) Wilson, R. M.; Elliott, J. C.; Dowker, S. E. P. *Am. Mineral.* **1999**, *84*, 1406.
(31) Berendsen, H. J. C.; Postma, J. P. M.; van Gunsteren, W. F.; Hermans, J. Interaction Models for Water in Relation to Protein Hydration. In *Intermolecular Forces*; Pullman, B., Ed.; Reidel: Dordrecht, The Netherlands, 1981.
(32) Kale, L.; Skeel, R.; Bhandarkar, M.; Brunner, R.; Gursoy, A.; Krawetz, N.; Phillips, J.; Shinozaki, A.; Varadarajan, K.; Schulten, K. *J. Comput. Phys.* **1999**, *151*, 283.
(33) MacKerell, A. D.; Bashford, D.; Bellott, M.; Dunbrack, R. L.; Evanseck, J. D.; Field, M. J.; Fischer, S.; Gao, J.; Guo, H.; Ha, S.; Joseph-McCarthy, D.; Kuchnir, L.; Kuczera, K.; Lau, F. T. K.; Mattos, C.; Michnick, S.; Ngo, T.; Nguyen, D. T.; Prodhom, B.; Reiher, W. E.; Roux, B.; Schlenkrich, M.; Smith, J. C.; Stote, R.; Straub, J.; Watanabe, M.; Wiórkiewicz-Kuczera, J.; Yin, D.; Karplus, M. *J. Phys. Chem. B* **1998**, *102*, 3586.
(34) Hauptmann, S.; Dufner, H.; Brickmann, J.; Kast, S. M.; Berry, R. S. *Phys. Chem. Chem. Phys.* **2003**, *5*, 635.
(35) Frisch, M. J.; Trucks, G. W.; Schlegel, H. B.; Scuseria, G. E.; Robb, M. A.; Cheeseman, J. R.; Montgomery, J. A., Jr.; Vreven, T.; Kudin, K. N.; Burant, J. C.; Millam, J. M.; Iyengar, S. S.; Tomasi, J.; Barone, V.; Mennucci, B.; Cossi, M.; Scalmani, G.; Rega, N.; Petersson, G. A.; Nakatsuji, H.; Hada, M.; Ehara, M.; Toyota, K.; Fukuda, R.; Hasegawa, J.; Ishida, M.; Nakajima, T.; Honda, Y.; Kitao, O.; Nakai, H.; Klene, M.; Li, X.; Knox, J. E.; Hratchian, H. P.; Cross, J. B.; Adamo, C.; Jaramillo, J.; Gomperts, R.; Stratmann, R. E.; Yazyev, O.; Austin, A. J.; Cammi, R.; Pomelli, C.; Ochterski, J. W.; Ayala, P. Y.; Morokuma, K.; Voth, G. A.; Salvador, P.; Dannenberg, J. J.; Zakrzewski, V. G.; Dapprich, S.; Daniels, A. D.; Strain, M. C.; Farkas, O.; Malick, D. K.; Rabuck, A. D.; Raghavachari, K.; Foresman, J. B.; Ortiz, J. V.; Cui, Q.; Baboul, A. G.; Clifford, S.; Cioslowski, J.; Stefanov, B. B.; Liu, G.; Liashenko, A.; Piskorz, P.; Komaromi, I.; Martin, R. L.; Fox, D. J.; Keith, T.; Al-Laham, M. A.; Peng, C. Y.; Nanayakkara, A.; Challacombe, M.; Gill, P. M. W.; Johnson, B.; Chen, W.; Wong, M. W.; Gonzalez, C.; Pople, J. A. *Gaussian 03*, revision B.02; Gaussian, Inc.: Pittsburgh, PA, 2003.
(36) Raffaini, G.; Ganazzoli, F. *Langmuir* **2004**, *20*, 3371.
(37) Isralewitz, B.; Baudry, J.; Gullingsrud, J.; Kosztin, D.; Schulten, K. *J. Mol. Graphics Modell.* **2001**, *19*, 13.
(38) Qiu, S. R.; Wierzbicki, A.; Salter, E. A.; Zepeda, S.; Orme, C. A.; Hoyer, J. R.; Nancollas, G. H.; Cody, A. M.; De Yoreo, J. J. *J. Am. Chem. Soc.* **2005**, *127*, 9036.
(39) Kessler, N.; Perl-Treves, D.; Addadi, L.; Eisenstein, M. *Proteins* **1999**, *34*, 383.
(40) DeOliveira, D. B.; Laursen, R. A. *J. Am. Chem. Soc.* **1997**, *119*, 10627.
(41) Shaw, W. J.; Long, J. R.; Dindot, J. L.; Campbell, A. A.; Stayton, P. S.; Drobny, G. P. *J. Am. Chem. Soc.* **2000**, *122*, 1709.
(42) Shaw, W. J.; Campbell, A. A.; Paine, M. L.; Snead, M. L. *J. Biol. Chem.* **2004**, *279*, 40263.
(43) Aizawa, T.; Koganesawa, N.; Kamakura, A.; Masaki, K.; Matsuura, A.; Nagadome, H.; Terada, Y.; Kawano, K.; Nitta, K. *FEBS Lett.* **1998**, *422*, 175.
(44) Keselowsky, B. G.; Collard, D. M.; Garcia, A. J. *Proc. Natl. Acad. Sci. U.S.A.* **2005**, *102*, 5953.